2016

Wettability Change by Pool Boiling of Nanofluids and Its Impact on Heat Transfer

Feini Zhang
University of Illinois at Urbana Champaign, United States of America, fzhang8@illinois.edu

Anthony Jacobi
University of Illinois at Urbana Champaign, United States of America, a-jacobi@illinois.edu

Wettability change by pool boiling of nanofluids and its impact on heat transfer

Feini ZHANG[*], Anthony M. JACOBI

University of Illinois at Urbana Champaign, Mechanical Science and Engineering,
Urbana, Illinois, USA
Phone:1(217)898-5671, E-mail: fnzhang28@gmail.com

* Corresponding Author

ABSTRACT

In refrigeration and air-conditioning systems, evaporator performance can be enhanced by avoiding dry-out of the tube wall. There are a myriad of other multiphase systems that can benefit from enhanced surface wetting. Using nanofluid boiling nanoparticle deposition (NBND), surface wettability can be enhanced significantly due to the formation of a porous layer that modifies liquid spreading. This paper will present an investigation of surfaces modified by nanofluid boiling using various types of aqueous aluminum oxide nanofluids nanofluids. Scanning Electronic Microscopy (SEM) images show the growth of aluminum oxide hydroxide on the aluminum substrate, which enhances affinity with water, and the micro-structures introduced by nanoparticle deposition. Atomic Force Microscopy (AFM) reveals the physics of the wettability enhancement by NBND on ultra-smooth substrates, which is described by Wenzel's wetting model. The impact of this change in wettability on boiling heat transfer will also be discussed with data from pool boiling experiment. These results will guide the design of nanoporous superhydrophilic coatings to enhance heat transfer from a surface science point of view.

1. INTRODUCTION

In air-conditioning and refrigeration applications, material surface wettability plays an important role in heat transfer devices when phase change occurs. For air-side dehumidification by an evaporator, higher fin surface wettability would prevent droplet bridging, enhance condensed water drainage, so reducing the air-side pressure penalty comparing to untreated fins. Research on hydrophilic surface coating on fins has shown up to 45% less pressure drop for louver fins and 15% for wavy fins (Hong & Webb, 1999). For plain fins, up to 40% reduction in pressure drop was reported by (Wang & Chang, 1998). It is reported that hydrophilic fins helps to double the j/f factor comparing to hydrophilic ones(Liu & Jacobi, 2009). Besides enhancing air-side thermal-hydraulic performance, the refrigerant side heat transfer can also benefit from the better wetting on surfaces. This includes falling film evaporation in shell-and-tube heat exchangers, which is often used for charge reduction in chiller systems. In such applications, dry-patches on the bottom tube surfaces is a problem especially for low Reynolds number cases. It has been reported that surface wettability enhancement would help to stabilize the thin liquid film on the tubes to dramatically enhance heat transfer at Reynolds number below 200 (Takata et al., 2000). Also observed from a hydrophilic coating was a significantly pressure drop reduction during flow boiling in a 5 mm wide minichannel, in compare with the hydrophobic coating. (Phan et al., 2011). Superhydrophilic surface are often found to effectively enhance the critical heat flux (CHF) in pool boiling experiments, and are considered in theoretical models.(Takata et al., 2003; Kandlikar, 2001)

2. WETTING THEORY

Because of the merits stated above, surface treatments that enhances wettability is an active area of research. Young's contact angle model (Eqn. 1) suggests that change of chemistry on interfaces would have a direct influence on the wetting behaviorr. As a result, chemical treatments such as plasma treatment, polymer coating and TiO_2 with UV light can be applied on large surface areas to enhance the wettability of heat transfer surfaces.(Min et al., 2000; G. r. Kim et al., 2003; Takata et al., 2003) However, hydrophilic surfaces are of high energy, which tent to absorb contaminations easily(Long et al., 2015). Fortunately, theoretical wetting models suggests that topographical modification can be used
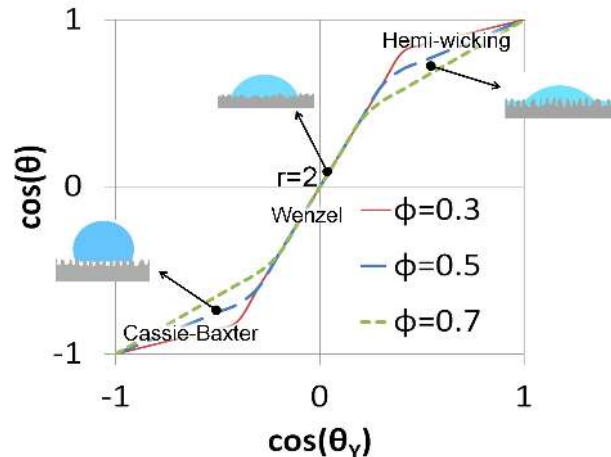
Figure 1: Cosine of apparent contact angle versus Young's contact for varies surface topography.

for better wetting behavior. If the cosine of contact angle is used to represent the wettability of a surface, then Figure 1 exhibits the effect of surface roughness r and solid fraction Φ in determining the wetting states, described by Wenzel's model (Eqn. 2), Cassie-Baxter's model (Eqn. 3) and the hemi-wicking model (Eqn. 4)(Bico et al., 2002). Guided by the theory, many techniques utilizes micro/nano fabrication to precisely modify topographical, that results in a porous or even biporous surfaces, in order to enhance the wetting of liquids on solid surfaces(Coso et al., 2012; Chu et al., 2013; Xiao et al., 2013). However, for air-conditioning and refrigeration applications, those methods are not feasible or cost effective for mass production. One of the alternatives that is promising for real HVAC&R applications is depositing nanoparticles by nanofluid boiling. Such simple method has been studied and proven to significantly enhance surface wettability(S. J. Kim et al., 2006; Phan et al., 2009; Zhang & Jacobi, 2014). In this paper, an indeepth investigation of the surface after nanofluid boiling using atomic force microscope (AFM) and scanning electronic microscope (SEM) is reported, to reveal the underlying principle. This understanding can be used to guide the design of surface coating for heat transfer enhancement, and its potential applications in HVAC&R is discussed in this paper.

$$\cos(\theta_Y) = \frac{\gamma_{sv} - \gamma_{sl}}{\gamma_{lv}} \tag{1}$$

$$\cos(\theta) = r\cos(\theta_Y) \tag{2}$$

$$\cos(\theta) = \Phi_{sl}\big(\cos(\theta_Y) + 1\big) - 1 \tag{3}$$

$$\cos(\theta) = \Phi_{sv}\big(\cos(\theta_Y) - 1\big) + 1 \tag{4}$$

3. EXPERIMENTAL METHOD

3.1 Nanofluid Pool Boiling

The nanofluid boiling experiment was done on by heating an aluminum sample block located at the bottom of the pool. The boiling experiment was done on surfaces of varies roughness and nanofluids of varies particle sizes and concentrations. The experimental parameter space is listed Table 1. All pool boiling processes has been done at a heat flux of $140\pm5\text{kW/m}^2$, and kept boiling for 10 minutes. Figure 2 shows the setup of the pool and the specimen heating section. A K type thermocouple is inserted at the center of the vessel to measure the temperature of the pool. The heating/boiling section is located at the bottom of the pool. An aluminum specimen of size 2 cm × 2 cm × 9 cm is insulated by PTFE. Two K type thermocouples were inserted into the small holes in the specimen, 6 mm below the

top surface. A ceramic heater of 2 cm × 2 cm area is located under the aluminum specimen. The top surface of the heater and the bottom surface of the specimen is firmly in contact with each other, secured by the force of the spring underneath the heater. The heater is insulated by PEEK. DC current was supplied to the heater by a power supply (Agilent Technologies N5771A). During the boiling process, LabVIEW recorded the current and voltage of the heater, which was then used to calculated the heat flux by equation 5, in which "Area" is 2 cm × 2 cm. Also recorded were the temperature of the specimen and the boiling pool. The specimen temperature was utilized to reduce the boiling surface temperature by Fourier's law of conduction, as shown in equation 6, where the δ is the distance between the thermocouple hole and top specimen surface (6 mm) and k is the thermal conductivity of AA6061 (16 W/mK). The heat transfer driving potential ΔT is the difference between pool temperature T_{pool} and the specimen top surface temperature T_w (equation 7). With the above parameters calculated, heat transfer coefficient can be easily found using equation 8.

After the nanofluid boiling nanoparticle deposition process, the specimen was removed carefully from the bottom of the pool, ready for wettability characterization.

$$q'' = \frac{IU}{Area} \tag{5}$$

$$T_w = T_{TC} - \frac{q''\delta}{k} \tag{6}$$

$$\Delta T = T_w - T_{pool} \tag{7}$$
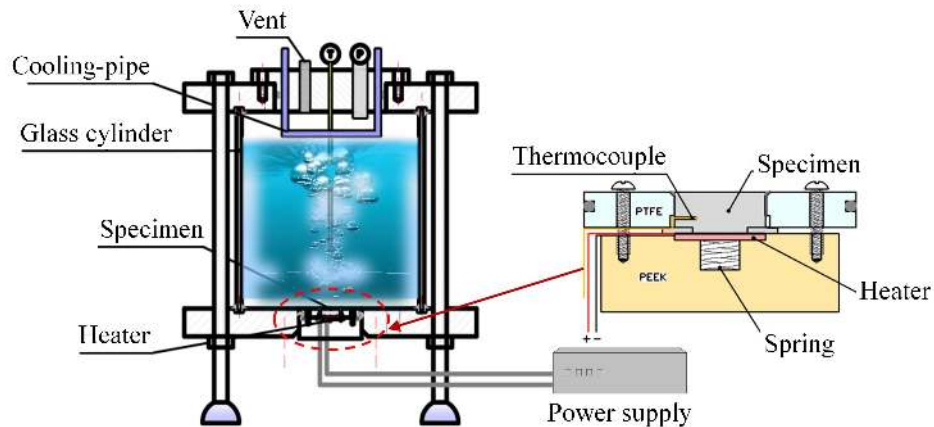
$$h = \frac{q''}{\Delta T} \tag{8}$$

Figure 2: Schematics of the boiling pool and the heating section located at the bottom.

3.2 Surface Wettability Analysis

Surface wettability is characterized by sessile droplet experiments using a goniometer (CAM2008). During the experiment, a droplet of about $5\mu L$ was placed on the specimen surface. The side-view of the droplet was recorded by a camera. The shape of the droplet was analyzed by the software using Young-Laplace equation.

Table 1: Experimental conditions for the boiling of 50 nm Al$_2$O$_3$ aqueous nanofluid on aluminum substrates

Nanoparticle size (nm)	0.01 wt% (0.0025 vol%)	0.1 wt% (0.025 vol%)	1 wt% (0.25 vol%)
13	-	-	Ultra-smooth
50	Ultra-smooth	Ultra-smooth	Ultra-smooth
50	Smooth	Smooth	Smooth
50	Rough	Rough	Rough
300	-	-	Ultra-smooth

3.3 Topography Analysis

Topography of the specimens were characterized by profilometry, AFM and SEM. Arithmetic roughness factor Ra is calculated from profilometer scan data. The Ra of ultra-smooth, smooth and rough substrates were found to be $0.01\pm0.01\mu$m, $0.27 \pm0.05\mu$m and $1.2 \pm0.1\mu$m, respectively. Eventhough the resolution of profilometry is relatively low, the profilometer can measure highly roughened surfaces. Roughness factor r can be estimated by the use of AFM, since such method is much more sensitive and accurate in capturing the nano-scale structures. AFM can give higher resolution, however, at the expense of its range of measurement. The AFM used here is Asylum Cypher, which has a limited Z direction measurement of less than 5 µm. The height difference from "peak" to "valley" on a surface must be well within that limit for the AFM to work properly. Rough surfaces, especially after nanofluid boiling, are challenging for AFM. As a result, so far, only the AFM result of specimen with ultra-smooth substrate is obtained. SEM images were obtained to qualitatively understand the result of the nanofluid boiling nanoparticle deposition process.

4. RESULTS AND DISCUSSION

4.1 Pool Boiling Heat Transfer

The boiling heat transfer coefficient of the nanofluid boiling process was reduced from the temperature and heat flux data. Figure 3 shows the result for varies nanoparticle concentrations of 50 nm Al$_2$O$_3$ aqueous nanofluid, and the data are grouped by substrate roughness. The horizontal axis in log scale, represents nanoparticle concentration by weight percentage, and the left end of the axis represents pure water boiling cases. It is known that roughness has an impact on boiling process because of its direct relationship with cavities and nucleation. The rough surface has higher heat transfer coefficient, because it has more surface area and active cavities in this study. Interesting to notice is that, there is a relationship between the nanoparticle concentration and the boiling heat transfer coefficient. Heat transfer tends to be enhanced by low or medium concentration nanofluids, while higher concentration of nanoparticle in the fluid deteriorates heat transfer. This trend is general for all roughness types of substrates (initial boiling surfaces). The phenomenon has to do with the tread off between the positive aspects of nanofluid boiling nanoparticle deposition: creation of some active nucleation cavities and the enhanced surface wettability; and the negative aspects of nanofluid boiling nanoparticle deposition: filling up of some active cavities and the added conductive heat transfer resistance by the accumulation of the particle deposition. Such effect is complicated and not very well understood. However, the investigation of surface topography and wettability after nanofluid boiling could give some insight to this sophisticated problem.

4.2 Surface Analysis

SEM images and contact angle of a ultrasmooth substrate is displayed in Figure 4. As can be seen, a reduction of contact angle from 93° to 47° indicates an enhancement in wettability of the surface boiled in pure water. This is a result of the production of boehmite or aluminum oxide hydroxide by aluminum and hot water reaction (Vedder & Vermilyea, 1969). The chemical nature of hydroxyl surface increases the affinity to water. The nano-grass structure of the boehmite adds nano-scale roughness. The above two factors both enhances water wettability of the surface. However, this is not enough for the purpose of heat transfer enhancement or pressure drop reduction. Note from Figure 4, the surface with the highest wettability (lowest contact angle of 22°) is the one after boiling in nanofluid. Nanoparticle deposition during the nanofluid boiling process results in a nano/micro hierarchical bi-porous structure. Such structure not only has the same chemical affinity to water as those pure water treated surface, but also introduces
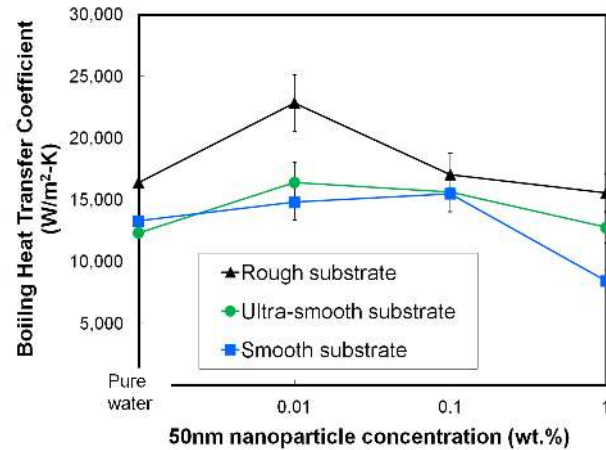
Figure 3: Heat transfer coefficient versus nanoparticle concentration during nanofluid boiling on ultra-smooth, smooth and rough aluminum surfaces. The nanoparticle in the fluid is 50 nm Al$_2$O$_3$.

the micro-scale roughness that enhances wettability.

Quantitative topography analysis is done by AFM scan. Its data can be used to estimate the roughness factor of the surface. For an ultra-smooth substrate boiled in 50 nm Al$_2$O$_3$ 1 wt% nanofluid. The total scan area is 12.2 μm^2 on a 3×3 μm^2 surface, which gives a roughness factor:

$$r = \frac{\text{total area}}{\text{projected area}} = \frac{12.2 \ \mu\text{m}^2}{9 \ \mu\text{m}^2} = 1.356 \tag{9}$$

Assuming that the wetting state of water on such surface can be described by Wenzel model (eqn. 2), then the roughness factor can also be derived from the contact angle of the surface over that of a pure water boiled surface (since both surfaces are covered by boehmite), that:

$$r = \frac{\cos(22°)}{\cos(44°)} = 1.360 \tag{10}$$

This implies a good agreement to the Wenzel state of wetting.

The nanoparticle deposition deposition process has been applied on a piece of fin for a plain fin design of heat exchanger. Because of the contaminations and oil residue, the contact angle was 95° (Figure 5), which means the surface is hydrophobic. Note that the fin surfaces are anisotropic in topography. There is certain texture formed during its manufacturing process. After the deposition of nanoparticles, wettability is significantly enhanced, showing a contact angle of only 28°, and the surface become more isotropic.

If the coating was to be applied on fins to enhance their wettability, the hight of a droplet on the fin surface would be a parameter that would affect the optimization of fin spacing. The higher the wettability, the lower the hight of a droplet, so the less the fin pitch could be. Wetting of rougher surfaces with a porous coating might be in the Hemi-wicking mode. Eventhough the surface solid fraction Φ_{sv} is very difficult to determine, especially on a randomly structured surface as the ones studied here, the imbibition effect or the wicking process can be observed by wetting experiments. The photo at the bottom right of Figure 6a demonstrate such observation from top view of the spreading process. Using larger size nanoparticles for the coating process results in a highly wettable surface exhibiting the thinnest liquid film (Figure 6b). Imbibition effect is involved in the fast spreading of liquid water on this surface, which contributes to the high apparent wettability of this surface. However, larger particle sized also results in a thicker coating, which is undesirable. The 13 nm particle size nanofluid and the 50 nm particle size nanofluid results in much thinner coatings, while the wettability is high enough. A 5μL fluid on its surface is less than 0.7 mm in height. If such coatings were applied on the fin surface of an evaporator in air-conditioning unit. The fin pitch design can be half of those designed for uncoated fins. If the fin pitch is kept the same, a significant reduction in pressure drop can be anticipated.
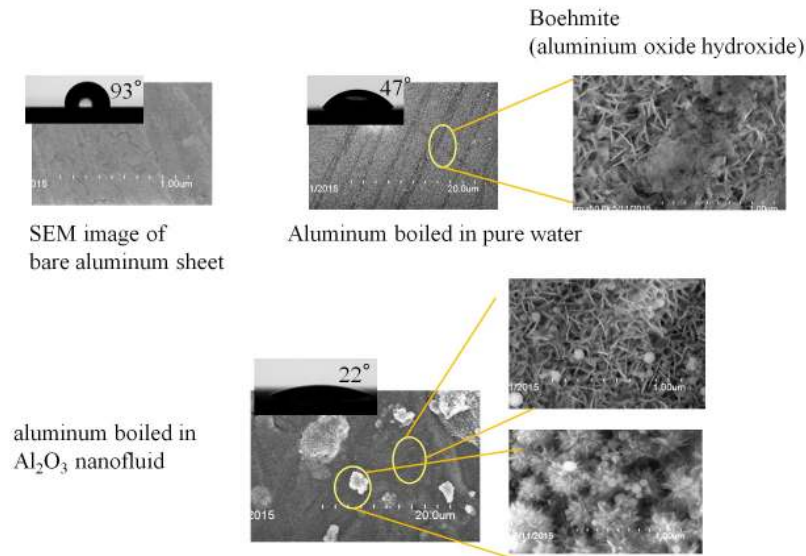
Figure 4: SEM images of ultrasmooth surfaces before and after boiling in pure water or 50 nm Al$_2$O$_3$ nanofluid, and their water contact angles.
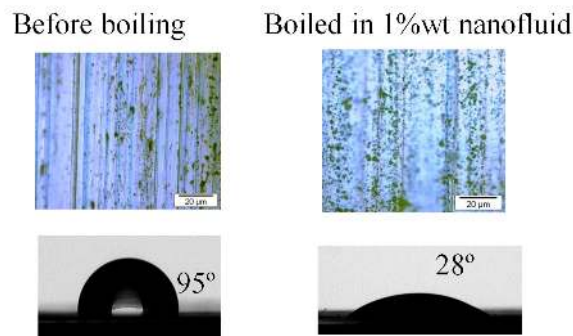
Figure 5: Fin surace strucure and wettability, before and after 50 nm Al$_2$O$_3$ nanofluid boiling nanoparticle deposition.

5. CONCLUSIONS

- Nanofluid boiling heat transfer on surfaces of different roughness indicated the complexity of this process, which involves coupled topography and chemistry change of the surface, that leads to a change in wettability.
- Nanoparticles deposition by boiling is a simple one step approach, that dramatically enhances surface wettability. The resulting surface wettability is related to the size of nanoparticle in the nanofluid.
- Surface analysis provided fundamental understanding of wettability changes by nanofluid boiling nanoparticle deposition. Based on the understanding, the exploration of its application on fin design provides a guidance to the utilization of this surface wettability treatment for heat exchangers.
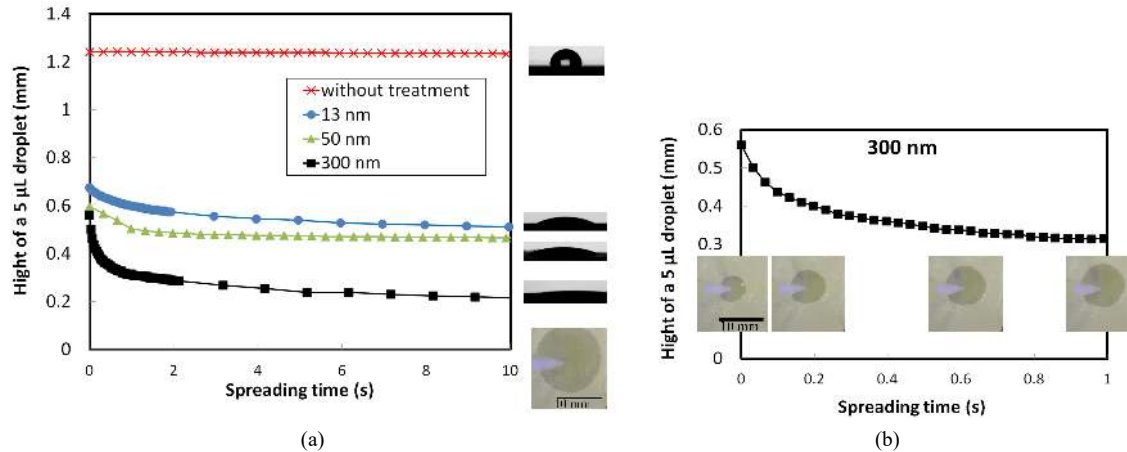
Figure 6: Spreading of water on the surfaces: (a) height versus time during the spreading on surfaces boiled in nanofluids with varies particle sizes with side view photos,(b) the first second of water spreading process on the surface boiled in 300nm nanofluid with top view photos

NOMENCLATURE

h	heat transfer coefficient	(W/m^2K)
I	current	(Amp)
k	thermal conductivity	(W/mK)
q''	heat flux	(kW/m^2)
r	roughness factor	(-)
Ra	arithmetic roughness	(μm)
T	temperature	(Celsius)
U	voltage	(Volt)
vol	by volume	(-)
wt	by weight	(-)
γ	interfacial energy, surface tension	(mN/m)
δ	distance	(m)
θ	apparent contact angle	(degree)
θ_Y	Young's contact angle	(degree)
Φ	solid fraction	(-)

Subscript

lv	liquid vapor interface
sl	solid liquid interface
sv	solid vapor interface
TC	thermocouple measurement
w	solid wall surface

REFERENCES

Bico, J., Thiele, U., & Quéré, D. (2002, 7/9). Wetting of textured surfaces. *Colloids and Surfaces A: Physicochemical and Engineering Aspects*, *206*(1–3), 41-46.

Chu, K. ., Joung, Y. S., Enright, R., Buie, C. R., & Wang, E. N. (2013). Hierarchically structured surfaces for boiling critical heat flux enhancement. *Applied Physics Letters*, *102*(15).

Coso, D., Srinivasan, V., Lu, M. ., Chang, J. ., & Majumdar, A. (2012). Enhanced heat transfer in biporous wicks in the thin liquid film evaporation and boiling regimes. *Journal of Heat Transfer*, *134*(10).

Hong, K., & Webb, R. L. (1999). Performance of dehumidifying heat exchangers with and without wetting coatings. *Journal of Heat Transfer*, *121*(4), 1018-1026.

Kandlikar, S. G. (2001). A theoretical model to predict pool boiling chf incorporating effects of contact angle and orientation. *Journal of Heat Transfer*, *123*(6), 1071-1079.

Kim, G. r., Lee, H., & Webb, R. L. (2003). Plasma hydrophilic surface treatment for dehumidifying heat exchangers. *Experimental Thermal and Fluid Science*, *27*(1), 1-10.

Kim, S. J., Bang, I. C., Buongiorno, J., & Hu, L. W. (2006). Effects of nanoparticle deposition on surface wettability influencing boiling heat transfer in nanofluids. *Applied Physics Letters*, *89*(15).

Liu, L., & Jacobi, A. M. (2009). Air-side surface wettability effects on the performance of slit-fin-and-tube heat exchangers operating under wet-surface conditions. *Journal of Heat Transfer*, *131*(5), 1-9.

Long, J., Zhong, M., Zhang, H., & Fan, P. (2015, 3/1). Superhydrophilicity to superhydrophobicity transition of picosecond laser microstructured aluminum in ambient air. *Journal of colloid and interface science*, *441*(0), 1-9.

Min, J., Webb, R. L., & Bemisderfer, C. H. (2000). Long-term hydraulic performance of dehumidifying heat-exchangers with and without hydrophilic coatings. *HVAC and R Research*, *6*(3), 257-272.

Phan, H. T., Caney, N., Marty, P., Colasson, S., & Gavillet, J. (2009). Surface wettability control by nanocoating: The effects on pool boiling heat transfer and nucleation mechanism. *International Journal of Heat and Mass Transfer*, *52*(23-24), 5459-5471.

Phan, H. T., Caney, N., Marty, P., Colasson, S., & Gavillet, J. (2011). Flow boiling of water in a minichannel: The effects of surface wettability on two-phase pressure drop. *Applied Thermal Engineering*, *31*(11-12), 1894-1905.

Takata, Y., Hidaka, S., Cao, J., Tanaka, K., Masuda, M., Ito, T., … M.Shimohigoshi (2000). Boiling and evaporation from a superhydrophilic surface. *Thermal Science and Engineering*, *8*(6), 33-41.

Takata, Y., Hidaka, S., Masuda, M., & Ito, T. (2003). Pool boiling on a superhydrophilic surface. *International Journal of Energy Research*, *27*(2), 111-119.

Vedder, W., & Vermilyea, D. A. (1969). Aluminum + water reaction. *Transactions of the Faraday Society*, *65*, 561-584.

Wang, C.-C., & Chang, C.-T. (1998, 10). Heat and mass transfer for plate fin-and-tube heat exchangers, with and without hydrophilic coating. *International Journal of Heat and Mass Transfer*, *41*(20), 3109-3120.

Xiao, R., Maroo, S. C., & Wang, E. N. (2013). Negative pressures in nanoporous membranes for thin film evaporation. *Applied Physics Letters*, *102*(12). (Cited By :5)

Zhang, F., & Jacobi, A. M. (2014, 14 July 2014 through 17 July 2014). Nanoparticle deposition by boiling on aluminum surfaces to enhance wettability. In *15th international refrigeration and air conditioning conference at purdue.* Purdue University.

ACKNOWLEDGMENT